Taylor & Francis
Taylor & Francis Group

RESEARCH PAPER

ⓐ OPEN ACCESS | Check for updates

Bone marrow mesenchymal stem cells-derived exosomal microRNA-124-3p attenuates hypoxic-ischemic brain damage through depressing tumor necrosis factor receptor associated factor 6 in newborn rats

Weijie Min[#], Yina Wu[#], Yibin Fang[#], Bo Hong, Dongwei Dai, Yu Zhou, Jianmin Liu, and Qiang Li[*]

Changhai Stroke Center, Changhai Hospital, Second Military Medical University, Shanghai China

ABSTRACT

Mesenchymal stem cells (MSCs)-derived exosomes (Exo) are beneficial in the use of brain damages. Restrictively, the mechanism of Exo expressing miR-124-3p in hypoxic-ischemic brain damage (HIBD) is not completely comprehended. Thereupon, this work was put forward to reveal the action of bone marrow MSCs-derived Exo (BMSCs-Exo) expressing miR-124-3p in the illness. BMSCs were isolated and transfected with miR-124-3p agomir. Then, BMSCs-Exo were extracted and identified. The newborn HIBD rats were injected with miR-124-3p-modified BMSCs-Exo or tumor necrosis factor receptor associated factor 6 (TRAF6)-related vectors. Next, neurological functions, neuron pathological and structural damages, oxidative stress and neuronal apoptosis were observed. miR-124-3p and TRAF6 expression was tested, along with their targeting relationship. miR-124-3p was down-regulated, and TRAF6 was up-regulated in newborn HIBD rats. miR-124-3p targeted TRAF6. BMSCs-Exo improved neurological functions, alleviated neuron pathological and structural damages, suppressed oxidative stress and reduced neuronal apoptosis in newborn HIBD rats, whereas BMSCs-Exo-mediated effects were enhanced by restoring miR-124-3p. Silencing TRAF6 attenuated HIBD in newborn rats, but overexpression of TRAF6 reversed the protective role of miR-124-3p-overexpressing BMSCs-Exo. This work makes it comprehensive that up-regulated exosomal miR-124-3p ameliorates HIBD in newborn rats by targeting TRAF6, which replenishes the potential agents for curing HIBD.

Graphical Abstract
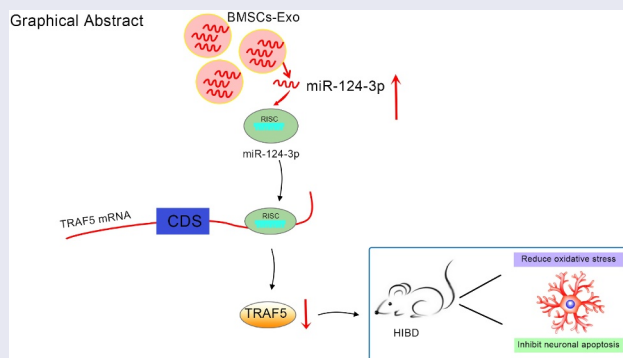
Introduction

Hypoxic-ischemic brain damage (HIBD) is the result of hypoxia-ischemia in the uterus, disturbing energy supply of fetal brain cells and further damaging brain metabolism [1]. Cell respiration interruption and abnormal metabolism lead to oxidative stress and the generation of free radicals, which induce inflammatory factors, destroy the blood–brain barrier and ultimately cause secondary brain damage [2]. Surviving HIBD infants usually further suffer from mental retardation, cerebral palsy and other dysfunctions in the long term [3]. Though

CONTACT Jianmin Liu ✉ Liujianmin1999@163.com 🖃 Changhai Stroke Center, Changhai Hospital, Second Military Medical University, Changhai Road 168, Shanghai 200433, China. **Tel**+86-02131161796; Qiang Li ✉ Liqiang19991@outlook.com 🖃 Changhai Stroke Center, Changhai Hospital, Second Military Medical University, Changhai Road 168, Shanghai, 200433, China
*These authors are co-corresponding authors.

#These authors are co-first authors.

🖃 Supplemental data for this article can be accessed here.

erythropoietin, hypothermia, xenon, hyperbaric oxygen and melatonin therapies are protective in treating HIBD, the efficacy is inferior to expectancy [4]. Thereupon, the requirement for applicable treatments for HIBD is a top task.

Exosomes (Exo) are endogenous vesicles that can transport therapeutic drugs and subdue biocompatibility, metabolic stability, blood–brain barrier penetrability and target specificity [5]. Exo are weaponed against ischemic brain damage by reducing infarct size [6]. Bone marrow mesenchymal stem cells (BMSCs)-derived extracellular vesicles have been shown to be protective against hypoxia-ischemia [7]. Exo delivery of miR-124 has been discovered to promote neurogenesis after ischemia [8], and miR-124 could improve neurological dysfunction recovery after neonatal HIBD [9]. Moreover, BMSCs-Exo containing miR-124-3p could attenuate neurological damage in spinal cord ischemia/reperfusion injury (IR/I) [10]. miR-124-3p is poorly expressed in the brain tissue of rats with permanent focal cerebral ischemia [11], and miR-124-3p could protect against kidney IR/I [12]. miR-124-3p could ameliorate IR/I in human cardiomyocytes by targeting tumor necrosis factor receptor associated factor 6 (TRAF6) [13]. TRAF6 is tightly connected with central nerve system diseases, such as neuropathic pain, stroke and traumatic brain injury [14]. TRAF6 expression is tended to increase in newborn male mice with HIBD [15]. There is a mechanistic study elucidating that TRAF6 down-regulation attenuates infarction, neurological deficits, oxidative stress and neuronal apoptosis in cerebral I/R [16]. Consulted from these prior studies, it deserves to explore that BMSCs-Exo expressing miR-124-3p function in newborn HIBD rats with the involvement with TRAF6.

Materials and methods

Ethics statement

This study has been approved by the ethics committee of Changhai Hospital and carried out in conformity with the recommendations in the Guidelines for the Care and Use of Laboratory Animals. Every effort has been made to minimize the suffering of animals.

Experimental animals

Newborn Sprague Dawley (SD) rats, aging 7 days old , were subjected to HIBD modeling. Male SD rats of specific pathogen-free grade, aging 4–5 weeks old were applied to isolate BMSCs. All rats were provided by Shanghai Dishi Biotechnology Co., Ltd. (Shanghai, China).

Culture and identification of BMSCs

SD rats were anesthetized to collect bilateral femurs, of which articular cartilage was removed. The medullary cavity, femur and tibia were repeatedly rinsed with phosphate buffered saline (PBS) to collect the red mixture. Then, the mixture was centrifuged at 1500 g/7 min, and the obtained pellets were resuspended in 5 mL complete medium (α-minimum essential medium + 10% fetal bovine serum (FBS) + 1% penicillin-streptomycin). Subsequently, the medium was renewed in half 24 h later and then renewed in total every 48–72 h. Cells of 70–80% confluence were detached by 0.25% ethylene diamine tetraacetic acid, followed by centrifugation at 1500 g/ 7 min and resuspension in complete medium. Finally, cells were seeded at 1:2 or 1:3 and observed under an inverted fluorescence microscope. Cells of passage 3 (P3) were identified by BD FACScan System (BD Biosciences, CA, USA) through flow cytometry. The antibodies included anti-CD90-PE, anti-CD44-PE, and anti-CD29-FITC, anti-rat-CD45-PE, anti-rat-CD34-PE (-Biolegend) [17–19].

The identified BMSCs were trypsinized and cultivated on 6-well culture plates at 3×10^6 cells/well to 60% confluence. Then, BMSCs were further incubated in a serum-free culture medium for 1 h and transfected with agomir NC or miR-124-3p agomir with Lipofectamine 2000 transfection reagent (Invitrogen, CA, USA). BMSCs-Exo were extracted by ultra-high speed centrifugation. The oligonucleotides plasmids were provided by GenePharma (Shanghai, China).

Extraction of BMSCs-Exo

After the BMSCs were cultured in the medium containing 10% exosome-free FBS for 48 h, the cells

were collected and treated by 300 × g centrifugation for 10 min and 2000 × g centrifugation for 10 min. The supernatant was filtered through a Steritop™ 0.22 μm sterile filter membrane (Millipore, MA, USA) and ultra-centrifuged at 150,000 g in a centrifuge (EPPENDORF, Germany) to collect the precipitate. Then, the exosomes were resuspended in PBS, centrifuged at 100,000 g for 1 h, and resuspended in 50–100 μL PBS and stored at −80℃ until the final volume was reduced to about 200 μL [20,21].

To detect the characteristics of the extracted exosomes, Western blot was used to detect the exsomal markers CD9 and CD81.

Transmission electron microscope (TEM)

Exo (10 μL) were diluted with an equal volume of PBS, dropped on a 2-mm copper net and counterstained with 2% phosphotungstic acid solution, which was followed by photography by a TEM [22,23].

Nanoparticle tracking analysis (NTA)

NTA of Exo was performed using NanoSight LM10 and NTA Version 2.3 Build 0034 software [23].

HIBD modeling on newborn rats

The newborn rats were anesthetized with isoflurane (2.5–3% for induction, 1.5–2% for maintenance) and processed with right common carotid artery occlusion. The right common carotid artery was isolated at the median carotid artery incision and ligated by 6/0 sterile threads at the distal and proximal ends. After 2 h, rats were placed in a hypoxic bottle and exposed to 8% oxygen and 92% nitrogen. After 1 h of hypoxia, the surviving rats were continuously reared. Rats in the sham group were treated with the right common carotid artery isolation but without ligation or hypoxic treatment [24].

Rat treatment

Newborn rats were randomly divided into nine groups (n = 12 in each group): (1) Sham group; (2) HIBD group (intraventricular injection of PBS 2 days after HIBD); (3) Exo group (intraventricular injection of BMSCs-Exo 2 days after HIBD); (4) Exo-agomir negative control (NC) group (Exo-agomir NC, intraventricular injection of agomir NC-transfected BMSCs-Exo 2 days after HIBD); (5) Exo-miR-124-3p agomir group (Exo + miR-124-3p agomir, intraventricular injection of miR-124-3p agomir-transfected BMSCs-Exo 2 days after HIBD); (6) scramble siRNA group (intraventricular injection of scramble siRNA vector 2 days after HIBD); (7) si-TRAF6 group (intraventricular injection of TRAF6 siRNA vector 2 days after HIBD); (8) Exo-miR-124-3p agomir + overexpression (oe)-NC group (intraventricular injection of miR-124-3p agomir-trasnfected BMSCs-Exo and empty vector 2 days after HIBD); (9) Exo-miR-124-3p agomir + oe-TRAF6 group (intraventricular injection of miR-124-3p agomir-trasnfected BMSCs-Exo and TRAF6 expression vector 2 days after HIBD). scramble siRNA vector, TRAF6 siRNA vector, empty vector and TRAF6 expression vector were purchased from Shanghai GenePharma Co.,Ltd. (Shanghai, China)[25].

Neurological function score

Neurological functions included spontaneous activity, spontaneous limb movement, forelimb movement, wire climbing, trunk touch and vibrio touch. The lower the score, the more serious the injury, the higher the score, the more normal.

Behavioral test: in order to test the motor coordination ability of each group of rats, we tested the foot failure of the rat-controlled model based on a reference [26]. Specifically, before modeling, rats were placed on a horizontal grid floor above the ground and allowed to walk for 2 min. The percentage of foot faults were recorded. On the 7th, 14th, 21st, and 28th d after modeling, the same test was performed [27]. When the foot malfunctioned, the rat could not step on the grid and fell off. The percentage of total foot failures for statistical analysis was recorded.

Tissue collection

At 7 days after HIBD, six mice were selected from each group. Rats were euthanized, and then the brain tissues were collected, part of which was

fixed with paraformaldehyde and prepared for histological staining. Another part stored at -80 was used for enzyme-linked immunosorbent assay (ELISA), reverse transcription quantitative polymerase chain reaction (RT-qPCR) and Western blot analysis.

Paraffin section preparation: Brain tissues were sequentially filled with 70%, 80%, 90%, 95% and 100% ethanol (2 h each), permeabilized in xylene (20–40 min) and embedded in paraffin (56–58°C). The coronal sections (5 μm) were obtained and baked at 65°C.

Hematoxylin-eosin (HE) staining

Dewaxed in xylene and previously hydrated with gradient ethanol, the sections were stained with hematoxylin for 8 min and with eosin for 2 min. Dehydrated in a conventional manner, the sections were sealed with resin and observed for the morphological changes under a high-power microscope [28,29].

Detection of oxidative stress-related indices

Brain tissue homogenate was prepared to test malondialdehyde (MDA) content and superoxide dismutase (SOD) activity using SOD (A001-3-2) and MDA (A003-1-2) detection kits (NanJing JianCheng Bioengineering Institute) [25].

Nitric oxide (NO) determination

NO level in the supernatant was measured by the detection kit (Beyotime, Shanghai, China). The supernatant was mixed with equal amounts of Griess reagents I and II. Absorbance value at 540 nm was read by Smart-Spec Plus spectrophotometer (Bio-Rad, CA, USA) [25].

DiI-labeled Exo in the hippocampus

Exo were labeled with a red fluorescent dye DiI (Celltracker CM-DiI, Invitrogen). After that, HIBD rats were euthanized after 24 h of Exo treatment, and the hippocampal tissue was fixed with 4% paraformaldehyde, dehydrated with 30% sucrose solution, embedded in Tissue-Tek O.C.T. Compound (SAKURA, USA), and solidified at −80°C. Finally, the tissue blocks were made into 5-μm frozen sections and observed under a fluorescence microscope. The number of red cells was counted through ImageProPlus 4.1 software in at least 10 fields [30].

Nissl staining

Brain sections were fixed overnight with 4% paraformaldehyde and then dehydrated by gradient sucrose, and frozen sectioned into 20 μm. The brain sections were treated with tar violet staining solution, put in 70%, 80%, 95% alcohol in sequence, and differentiated in a special color separation solution (1:1:1 absolute ethanol, chloroform, ether). The sections were immersed in 100% ethanol, permeabilized with xylene, sealed with gum, and observed with an optical microscope (OLYMPUS IX71, Olympus, Japan).

Transferase-mediated deoxyuridine triphosphate-biotin nick end labeling (TUNEL) staining

The baked sections at 60°C were dewaxed in xylene and dehydrated with gradient ethanol in TUNEL kits (Roche Diagnostic Systems, Inc., Branching, NJ, USA). Treated with proteinase K for 10 min, sections were reacted with TUNEL solution (1 h) and with 3% H_2O_2 methanol (10 min) and peroxidase solution (30 min). To proceed, sections were stained by diaminobenzidine and counterstained with hematoxylin, following gradient ethanol dehydration, xylene permeabilization and resin sealing. The cells with brown nucleus are apoptosis-positive cells, and those with blue nucleus are normal cells, and their number ratio was calculated [31].

RT-qPCR

Based on Trizol method, the extracted total RNA from brain tissues were dissolved in RNase-free water and tested for concentration and purification by a ND-1000 ultraviolet/visible spectrophotometer (NanoDrop Technologies Inc., Wilmington, USA). Complementary DNA obtained by reverse transcription of RNA was preserved at −20°C. Primer sequences were listed in Supplementary Table 1.

With the help of a real-time fluorescent qPCR instrument (TIB-8000, Taipplex, Fuzhou, China), qPCR was executed. U6 and glyceraldehyde-3-phosphate dehydrogenase (GAPDH) were loading controls for miR-124-3p and TRAF6, whose gene expression was calculated by $2^{-\Delta\Delta Ct}$ method[32,33].

Western blot assay

Brain tissues were homogenized and sonicated on ice. Obtained by centrifugation, the supernatant (aliquot of 20 μg/mg protein) was separated by sodium dodecyl sulfate polyacrylamide gel electrophoresis and transferred to a membrane. Next, the blocked membrane by 5% skim milk (pH = 7.4) was reacted with the primary antibodies TRAF6 (1:1000), B cell lymphoma 2 (Bcl-2; 1:1000), Bcl-2-associated X(Bax; ab199677, 1:1000, Abcam) and GAPDH (1:5000, Proteintech) overnight, and with the secondary antibody for 2 h. Visualized by a chemiluminescence instrument (ImageQuant LAS 4000mini, GE Healthcare, USA), gray values on the protein bands were measured with Image-J software and normalized to GAPDH [34].

Dual luciferase reporter gene assay

Bioinformatics software TargetScanHuman 7.2 (http://www.targetscan.org/vert_72/) predicted the binding site of miR-124-3p and TRAF6. Wild type (WT)-3′untranslated region containing miR-124-3p binding sites and its mutant fragments of TRAF6 were cloned into psiCHECK-2 vector (Promega, WI, USA). HEK-293 T cells were co-transfected with WT/MUT reporter plasmids and miR-124-3p agomir or agomir-NC for 48 h by HilyMax transfection reagent (Dojindo, Kumamoto, Japan). Luciferase activity was tested by Dual-Luciferase Reporter Assay System (Promega) [35].

Statistical analysis

All data were evaluated using SPSS 21.0 (IBM, NY, USA) statistical software. The measurement data were expressed as mean ± standard deviation. Discrepancy between two groups was assessed by independent sample t test while that among multiple groups by one-way analysis of variance (ANOVA), followed by Tukey's multiple comparisons test. Given that $P < 0.05$, statistical significance was set.

Results

Identification of BMSCs and BMSCs-Exo

It has been previously reported that BMSCs-Exo containing miR-124-3p can reduce the nerve damage to spinal cord IR/I [10] and miR-124-3p is low in the brain tissue of rats with permanent focal cerebral ischemia [11]. We wondered whether miR-124-3p from BMSCs-Exo protects neonatal rats from HIBD.

BMSCs were separated and identified: Primary BMSCs grew rapidly and adhered largely to the wall. The cell morphology gradually became spindle-shaped and densely arranged. BMSCs of P3 became uniform and grew in a whirlpool (Figure 1). After flow cytometry analysis, it was found that the cell surface characteristic markers CD90, CD44 and CD29 were positive, while CD34 and CD45 were negative (Figure 1), indicating that the extraction of BMSCs was successful.

Observed by TEM, the Exo were round membranous vesicles (Figure 1); NTA found that the Exo were 40–100 nm in diameter (Figure 1). Western blot assay determined that Exo expressed CD81 and CD9 (Figure 1).

Successful HIBD modeling in rats

miR-124-3p and TRAF6 expression in the brain tissues of newborn rats were tested using RT-qPCR and Western blot assay (Figure 2–b). It was witnessed that miR-124-3p expression trended toward a decrease while TRAF6 toward an increase in HIBD newborn rats.

Neurological function test and behavioral test on rats revealed that after HIBD modeling, the neurological score decreased (Figure 2) and the percentage of fault steps increased (Figure 2). HE staining observed that the brain tissue of the rats in the sham group was clearly structured, the neurons were arranged neatly, the morphology and structure were intact, the nucleus was intact without intercellular edema or inflammatory cell infiltration. The brain tissue of rats in the HIBD group showed typical ischemia-hypoxic changes,
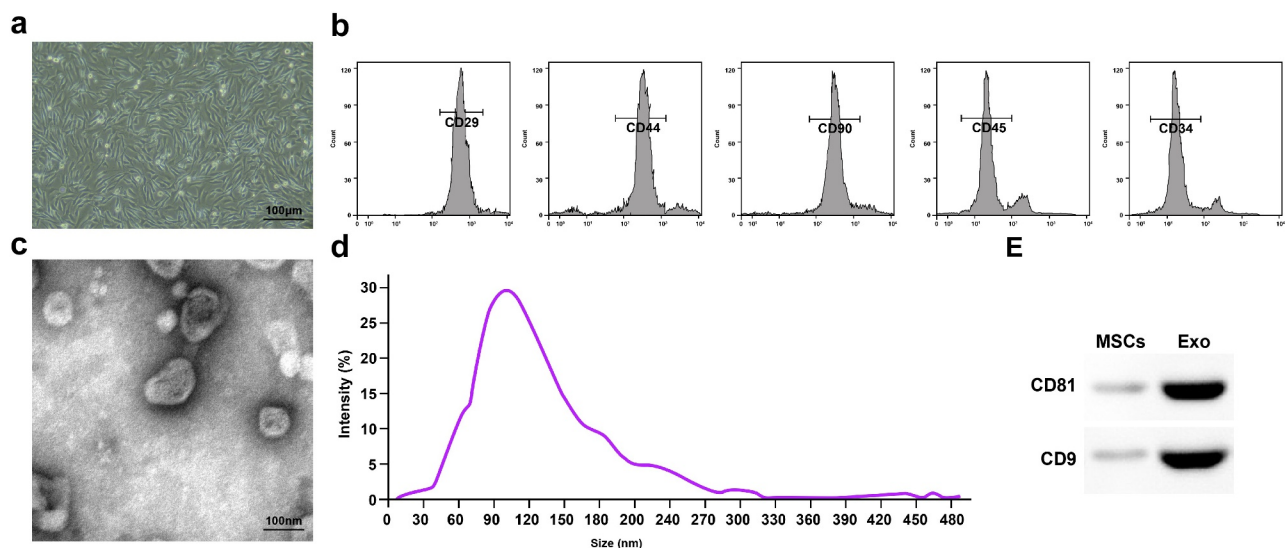
Figure 1. Identification of BMSCs and BMSCs-Exo. A. Morphology of BMSCs of P3; B. Analysis of surface markers by flow cytometry; C. TEM observed size and morphology of BMSCs-Exo; D. NTA of BMSCs-Exo; E. Western blot analysis of CD81 and CD9.
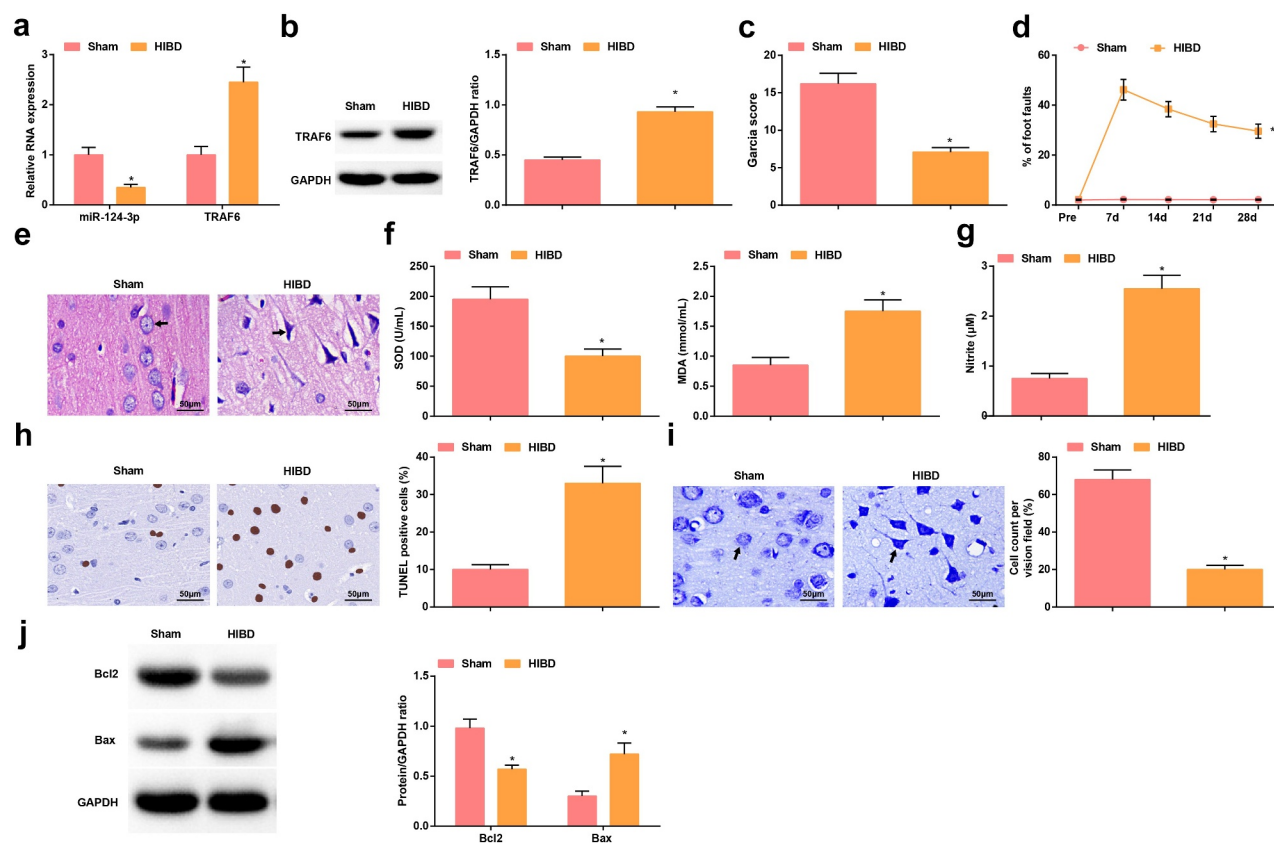

Figure 2. Successful HIBD modeling in rats. A. RT-qPCR detection of miR-124-3p and TRAF6 mRNA expression; B. Western blot detection of TRAF6 protein expression; C. Neurological function score of rats after HIBD; D. Behavioral function of rats after HIBD; E. HE staining; F. SOD and MDA levels of rats after HIBD; G. NO levels of rats after HIBD; H. TUNEL staining; I. Nissl staining; J. Bax and Bcl-2 protein expression of rats after HIBD; measurement data were expressed as mean ± standard deviation; * $P < 0.05$ vs. the Sham group.

nuclear pyknosis, loss of neuron nuclei in some areas, decreased number of neurons, swelling of neurons, and loose cytoplasm (Figure 2). The activity of SOD in the brain tissue of rats after HIBD modeling was impaired and the levels of MDA and NO were increased (Figure 2, g), the number of TUNEL-positive cells was increased, the number of normal neurons was decreased (Figure 2, i), Bcl-2 protein expression was reduced and Bax protein expression was increased (Figure 2). In summary, HIBD modeling was successful.

BMSCs-Exo improve HIBD in newborn rats

DiI labeled-Exo and unlabeled-Exo were injected into HIBD rats to explore the distribution of Exo in rat brain tissue, and PBS was used as a control. The results showed that no red fluorescence was observed in the hippocampus of the rats injected with PBS or Unlabeled-Exo, while red fluorescence was seen in the hippocampal tissue of rats injected with DiI labeled-Exo (Figure 3). Then, the experimental outcomes displayed that after treatment with Exo, neurological function scores were increased (Figure 3), the percentage of foot faults was reduced (Figure 3), cell edema and vacuole-like changes in brain tissues were attenuated, and the number of neuronal degeneration and necrosis was reduced (Figure 3). Moreover, Exo heightened SOD activity, suppressed MDA and NO levels (Figure 3, f), as well as decreased the number of TUNEL-positive cells, increased the number of normal neurons (Figure 3, h), elevated Bcl-2 protein expression and suppressed Bax protein expression (Figure 3).
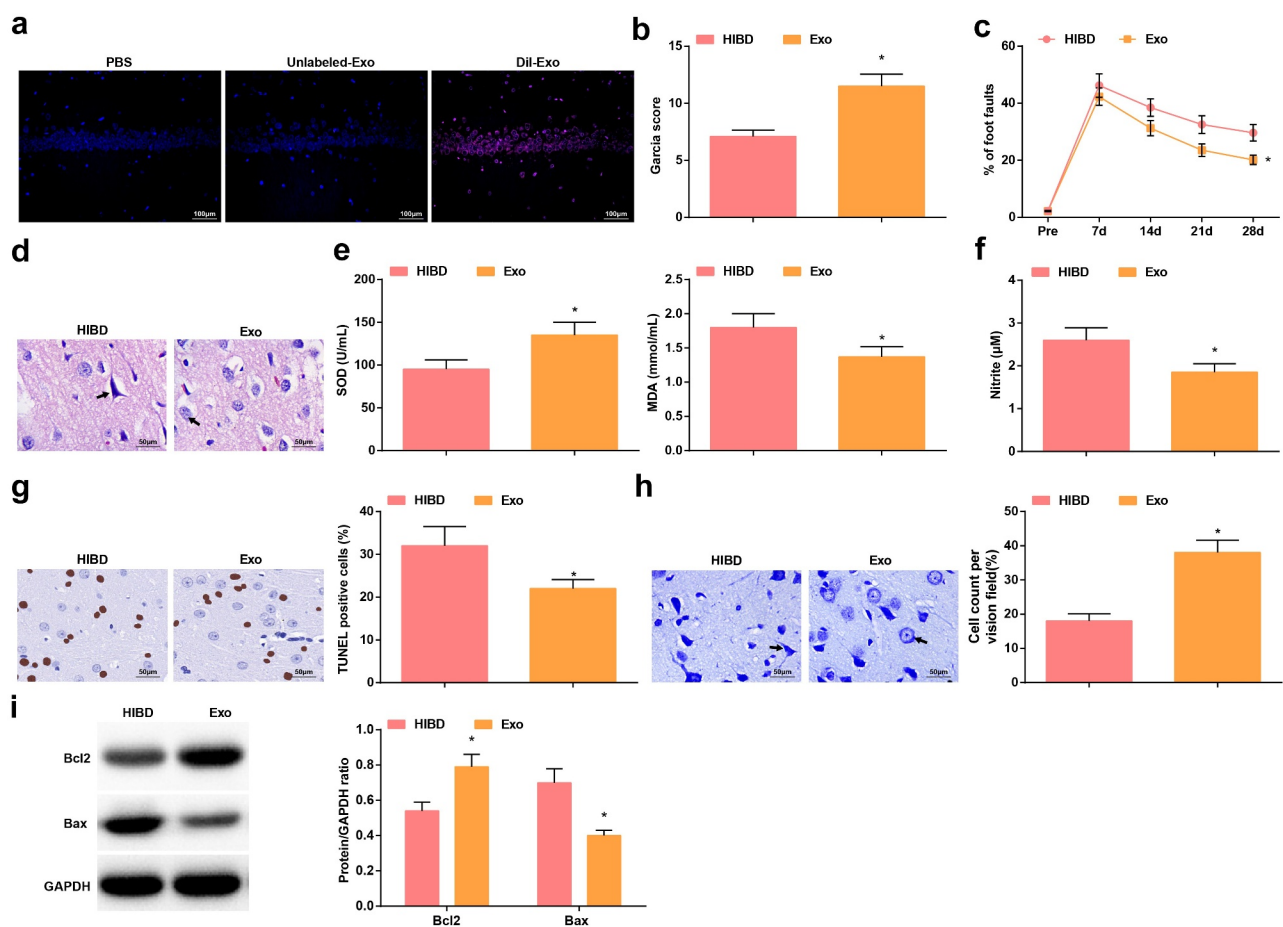

Figure 3. BMSCs-Exo improve HIBD in newborn rats. A. DiI-labeled Exo in the hippocampus of HIBD rats; B. Neurological function score of HIBD rats after injection with BMSCs-Exo; C. Behavioral function of HIBD rats after injection with BMSCs-Exo; D. HE staining; E. SOD and MDA levels of HIBD rats after injection with BMSCs-Exo; F. NO levels of HIBD rats after injection with BMSCs-Exo; G. TUNEL staining; H. Nissl staining; I. Bax and Bcl-2 protein expression in HIBD rats after injection with BMSCs-Exo; measurement data were expressed as mean ± standard deviation; * $P < 0.05$ vs. the HIBD group.
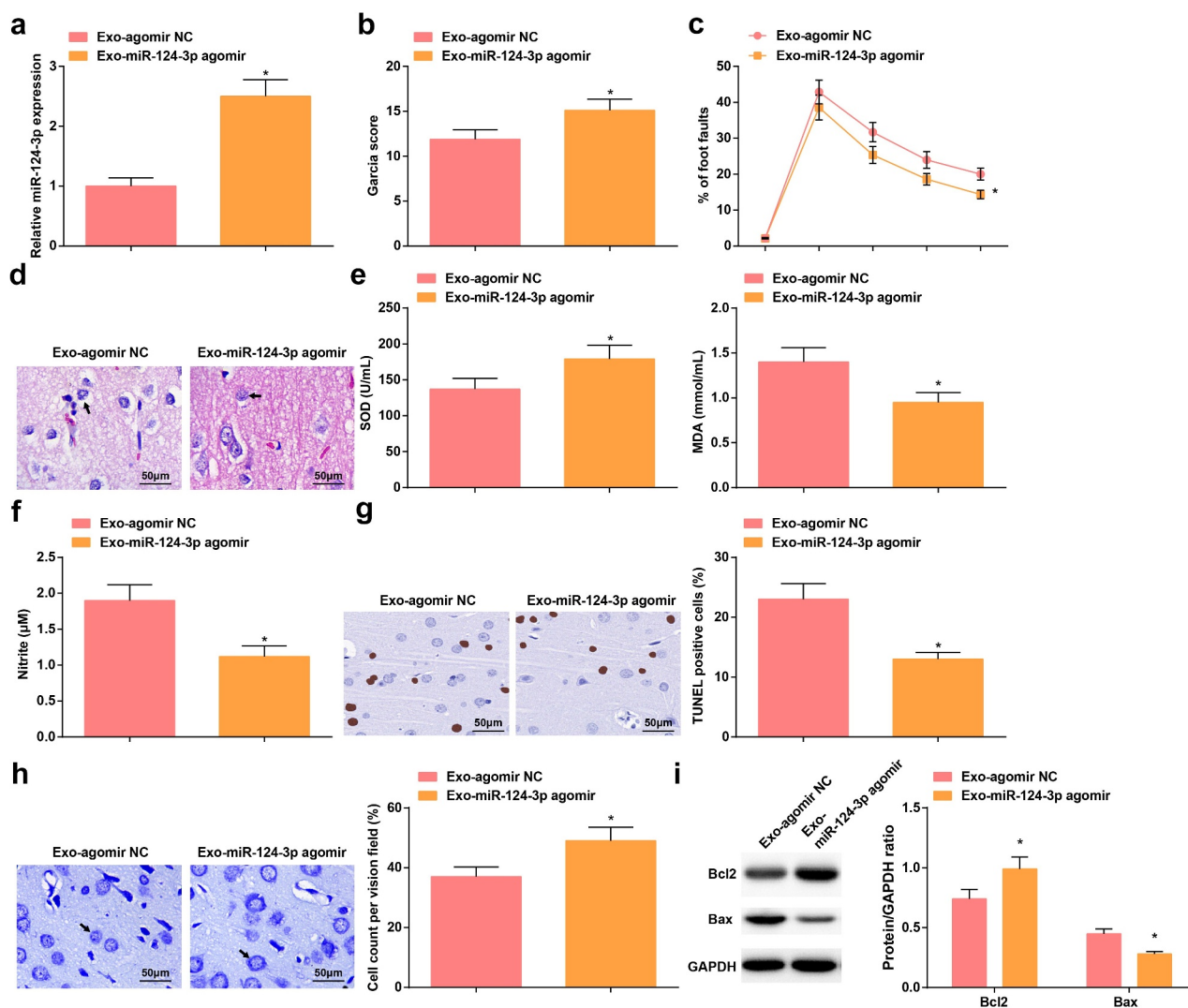
Figure 4. Up-regulated miR-124-3p further enhances the protective role of BMSCs-Exo on HIBD rats. A. miR-124-3p expression in HIBD rats after injection with Exo-miR-124-3p agomir; B. Neurological function score of HIBD rats after injection with Exo-miR-124-3p agomir; C. Behavioral function of HIBD rats after injection with Exo-miR-124-3p agomir; D. HE staining; E. SOD and MDA levels of HIBD rats after injection with Exo-miR-124-3p agomir; F. NO levels of HIBD rats after injection with Exo-miR-124-3p agomir; G. TUNEL staining; H. Nissl staining; I. Bax and Bcl-2 protein expression in HIBD rats after injection with Exo-miR-124-3p agomir; measurement data were expressed as mean ± standard deviation; * $P < 0.05$ vs. the Exo-agomir NC group.

Up-regulated miR-124-3p further enhances the protective role of BMSCs-Exo on HIBD rats

To investigate the effect of miR-124-3p on HIBD, Exo were extracted from BMSCs transfected by agomir NC and miR-124-3p agomir (Invitrogen) and injected into the lateral ventricle of HIBD rats. The success of injection was verified by RT-qPCR (Figure 4). Injection with Exo transmitting miR-124-3p agomir had greater protective effects on HIBD rats, as indicated by higher neurological function scores, reduced percentage of foot faults, alleviated pathological status in the brain tissue, and suppressed oxidative stress and neuronal

apoptosis in comparison to injection with Exo transmitting agomir NC (Figure 4–i).

miR-124-3p targets TRAF6

TargetScanHuman 7.2 predicted the binding site of miR-124-3p and TRAF6 (Figure 5). Dual-luciferase reporter gene assay showed that miR-124-3p agomir diminished the luciferase activity of TRAF6-WT (Figure 5), indicating that miR-124-3p could target TRAF6. Outcomes of RT-qPCR and Western blot displayed that in Exo extracted from BMSCs transfected with miR-124-3p agomir, TRAF6 mRNA and
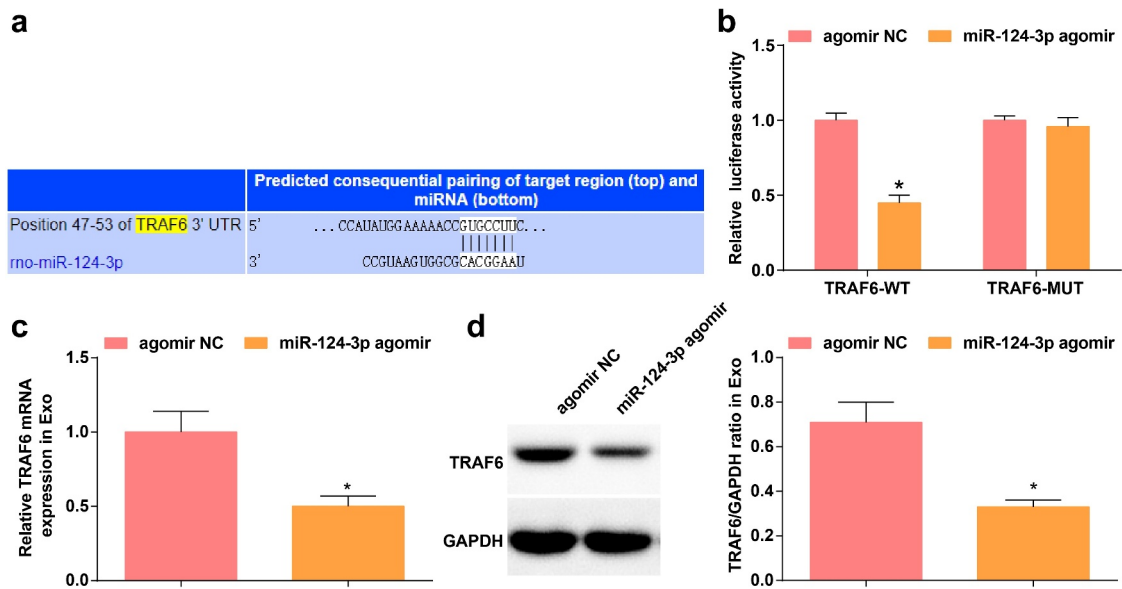
Figure 5. miR-124-3p targets TRAF6. A. Jefferson website predicted the binding site between TRAF6 and miR-124-3p; B. Dual luciferase reporter gene assay verified the targeting relationship between TRAF6 and miR-124-3p; C-D. RT-qPCR and Western blot analysis of TRAF6 expression in Exo; measurement data were expressed as mean ± standard deviation; * P < 0.05 vs. the agomir NC group.
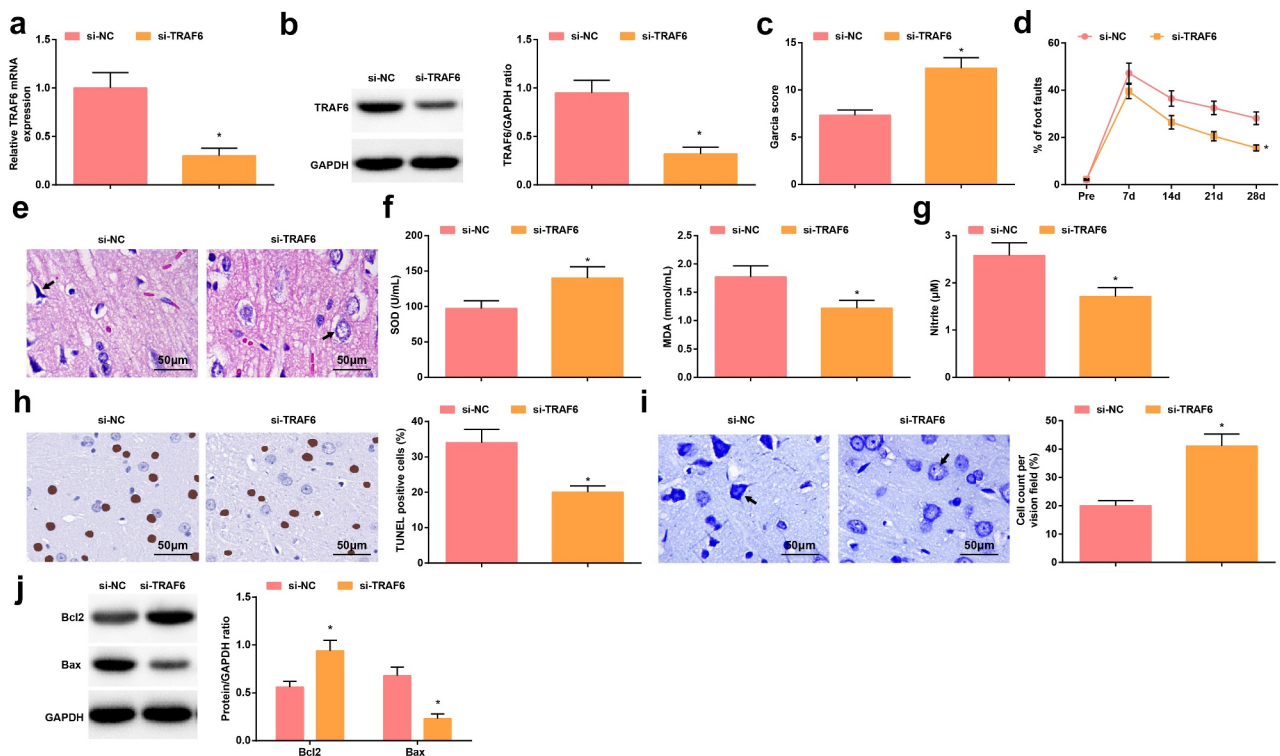

Figure 6. Depressing TRAF6 exerts protectively for rats with HIBD. A-B. RT-qPCR and Western blot analysis of TRAF6 expression in HIBD rats after injection with si-TRAF6; C. Neurological function score of HIBD rats after injection with si-TRAF6; D. Behavioral function of HIBD rats after injection with si-TRAF6; E. HE staining; F. SOD and MDA levels of HIBD rats after injection with si-TRAF6; G. NO levels of HIBD rats after injection with si-TRAF6; H. TUNEL staining; I. Nissl staining; J. Bax and Bcl-2 protein expression in HIBD rats after injection with si-TRAF6; measurement data were expressed as mean ± standard deviation; * P < 0.05 vs. the si-NC group.

protein levels were reduced in comparison to Exo extracted from BMSCs transfected with agomir NC (Figure 5, d).

Depressing TRAF6 exerts protectively for rats with HIBD

TRAF6 expression was successfully suppressed by injecting si-TRAF6 into HIBD rats (Figure 6, b). In response to the silencing of TRAF6, HIBD rats presented improved neurobehavioral functions, attenuated neuronal damage in the brain tissue, limited oxidative stress, increased number of normal neurons, and decreased number of TUNEL-positive neurons (Figure 6–j).

Elevating TRAF6 antagonizes miR-124-3p-mediated protection against HIBD in rats

The mechanism of miR-124-3p/TRAF6 in HIBD was further investigated by establishing Exo-miR-124-3p agomir + oe-NC group and Exo-miR-124-3p agomir + oe-TRAF6 group. It was verified that injection of oe-TRAF6 on the basis of Exo-miR-124-3p agomir injection elevated TRAF6 expression in HIBD rats (Figure 7, b). Then, it was recognized that the protective actions of Exo-miR-124-3p agomir regarding neurobehavioral functions, brain pathological damage, oxidative stress and apoptosis were all mitigated by oe-TRAF6 (Figure 7–j).
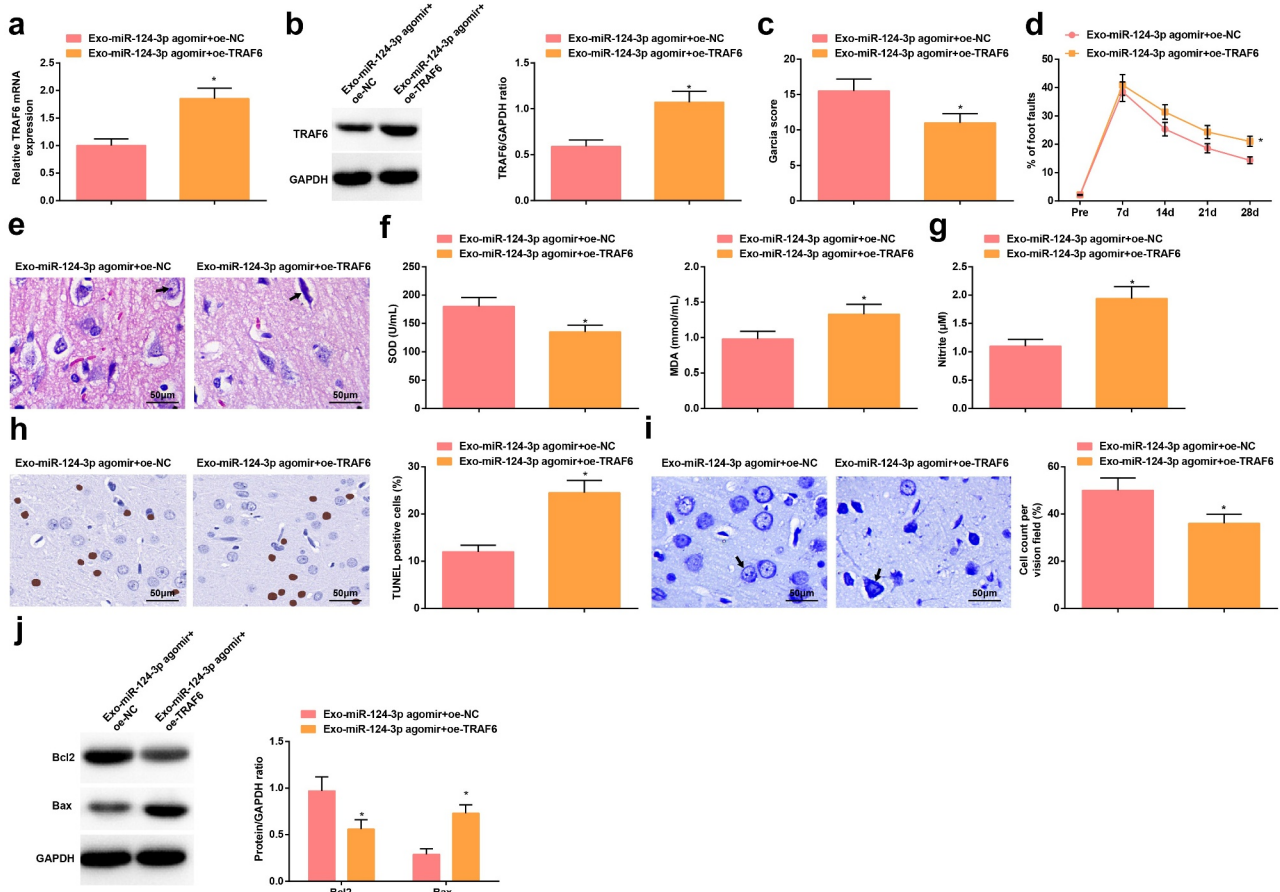

Figure 7. Elevating TRAF6 antagonizes miR-124-3p-mediated protection against HIBD in rats. A-B. RT-qPCR and Western blot analysis of TRAF6 expression in HIBD rats in rescue experiment; C. Neurological function score of HIBD rats in rescue experiment; D. Behavioral function of HIBD rats in rescue experiment; E. HE staining; F. SOD and MDA levels of HIBD rats in rescue experiment; G. NO levels of HIBD rats in rescue experiment; H. TUNEL staining; I. Nissl staining; J. Bax and Bcl-2 protein expression in HIBD rats in rescue experiment; measurement data were expressed as mean ± standard deviation; * $P < 0.05$ vs. the Exo-miR-124-3p agomir + oe-NC group.

Discussion

HIBD takes over a position in the overwhelming cause for neonatal death and permanent neurological disability [36]. This work was originated with regard to Exo transfer of miR-124-3p in HIBD through regulating TRAF6. Ultimately, it is delineated that exosomal miR-124-3p attenuates HIBD in newborn rats through repressing TRAF6.

Initially, BMSCs-Exo were injected into HIBD rats, and the findings disclosed that BMSCs-Exo attenuated HIBD by improving neurological functions, alleviating pathological and structural damages of neurons, inhibiting oxidative stress, depressing neuronal apoptosis and increasing the number of normal neurons. Conspicuously, human MSCs-Exo could down-regulate TRAF6 and have potential therapeutics in the treatment of I/RI [37]. Also, treatment with MSCs-Exo is effective in improving motor, learning and memory abilities in acute brain injury [38]. Intriguingly, umbilical cord stem cells-derived Exo have been proved to induce learning ability and functional recovery in perinatal brain injury [39]. Actually, Liu X *et al.* have implied that induction of BMSCs-Exo could repress inflammation and pyroptosis following cerebral IR/I [40]. On the other hand, MSCs-derived extracellular vesicles have been implicated in relieving fetal brain after hypoxia-ischemia [7], and administration with BMSCs-Exo generates the promoting effects on functional recovery and neuroprotection in rats with ischemic Stroke [41].

Critically, miR-124-3p expression was analyzed to be down-regulated in HIBD rats. For a comprehensive understanding of miR-124-3p-oriented mechanism in HIBD, Exo-transmitted miR-124-3p agomir was injected into HIBD rats, eventually promoting the protective actions of Exo in rats. A supportive research has elaborated that overexpressed miR-124-3p delivered by BMSCs-Exo could suppress apoptosis and nerve injury in spinal cord IR/I [10]. According to a former experiment, miR-124-3p expression is inhibited in the ischemic penumbra after permanent middle cerebral artery occlusion, and miR-124-3p agomir-induced miR-124-3p overexpression could narrow brain infarction [11]. Experimentally, restoring miR-124-3p could mitigate hypoxia/re-oxygenation (H/R)-induced apoptosis of cardiomyocytes [42]. Notably, miR-124-3p expression is suppressed in H/R-treated HK-2 cells, and inhibition of miR-124-3p results in impaired cell viability, as well as enhanced oxidative stress [12]. Evidenced by the current work, miR-124-3p overexpression could re-activate the viability and weaken the apoptosis of H/R-treated renal cells [43]. Experimentally, miR-124-3p is lowly expressed after traumatic brain injury [44], but overexpressed miR-124-3p transmitted by microglial Exo improves cognitive dysfunction induced by repetitive mild traumatic brain injury [45].

To proceed, our findings suggested that miR-124-3p targeted and inhibited TRAF6 expression. Further analysis of TRAF6 in HIBD manifested that TRAF6 was up-regulated in HIBD newborn rats and its knockdown protected rats from HIBD. In fact, the targeting relation between miR-124-3p and TRAF6 has been validated previously [13]. It is recorded that TRAF6 expression is impaired in HIBD, specifically in newborn male mice [15]. Similarly, heightened TRAF6 expression is stimulated by cerebral I/R and its down-regulation decreases neurological deficit scores and blocks oxidative stress and neuronal apoptosis [16]. Referring to a paper by Yujue Wang *et al.*, inhibiting TRAF6 can ameliorate cerebral I/R injury and reduce inflammation response [46]. Supplementary to this work, there is another research having revealing that repression of TRAF6 in part restrains brain damage and inflammation in cerebral ischemia injury [47].

Conclusion

Jointly, it is conspicuous that miR-124-3p is down-regulated in newborn rats with HIBD, and up-regulated exosomal miR-124-3p protects against HIBD in newborn rats by suppressing TRAF6, which replenishes a novel target for managing HIBD in infants. Restricted by the relatively small experimental scale, the results obtained are supposed to be validated in a large cohort.

Disclosure statement

No potential conflict of interest was reported by the author(s).

Funding

Consent for publication

The participant has consented to the submission of the case report to the journal.

Availability of data and material

The original contributions presented in the study are included in the article/Supplementary Material, and further inquiries can be directed to the corresponding author.

Authors' contributions

Jianmin Liu, Qiang Li and Bo Hong finished study design, Weijie Min, Yina Wu, Yibin Fan and Dongwei Dai finished experimental studies, Yu Zhou and Yibin Fang finished data analysis, Bo Hong and Qiang Li finished manuscript editing. All authors read and approved the final manuscript.

References

[1] Huang R, Zhang, J, Ren, SJ, et al. Effect of erythropoietin on Fas/FasL expression in brain tissues of neonatal rats with hypoxic-ischemic brain damage. Neuroreport. 2019;30(4):262–268.

[2] Vasiljevic B, Maglajlic-Djukic Svjetlana, S, Gojnic, M, et al. New insights into the pathogenesis of perinatal hypoxic-ischemic brain injury. Pediatr Int. 2011;53 (4):454–462.

[3] Yang L, Zhao H, Cui H. Treatment and new progress of neonatal hypoxic-ischemic brain damage. Histol Histopathol. 2020;35(9):929–936.

[4] Jiang Y, Bai, X, Li, TT, et al. COX5A over-expression protects cortical neurons from hypoxic ischemic injury in neonatal rats associated with TPI up-regulation. BMC Neurosci. 2020;21(1):18.

[5] Luo S, Du L, Cui Y. Potential therapeutic applications and developments of exosomes in parkinson's disease. Mol Pharm. 2020;17(5):1447–1457.

[6] Nalamolu KR, Venkatesh, S, Mohandass, A, et al. Exosomes treatment mitigates ischemic brain damage but does not improve post-stroke neurological outcome. Cell Physiol Biochem. 2019;52(6):1280–1291.

[7] Ophelders DR, Wolfs Tim, GAM, Jellema Reint, K, et al. Mesenchymal stromal cell-derived extracellular vesicles protect the fetal brain after hypoxia-ischemia. Stem Cells Transl Med. 2016;5(6):754–763.

[8] Yang J, Zhang, XF, Chen, XJ, et al. Exosome mediated delivery of miR-124 promotes neurogenesis after ischemia. Mol Ther Nucleic Acids. 2017;7:278–287.

[9] Xiong L, Zhou, H, Zhao, Q, et al. Overexpression of miR-124 protects against neurological dysfunction induced by neonatal hypoxic-ischemic brain injury. Cell Mol Neurobiol. 2020;40(5):737–750.

[10] Li R, Zhao, KC, Ruan, Q, et al. Bone marrow mesenchymal stem cell-derived exosomal microRNA-124-3p attenuates neurological damage in spinal cord ischemia-reperfusion injury by downregulating Ern1 and promoting M2 macrophage polarization. Arthritis Res Ther. 2020;22(1):75.

[11] Xu SY, Jiang, XL, Qian, L, et al. Role of rno-miR-124-3p in regulating MCT1 expression in rat brain after permanent focal cerebral ischemia. Genes Dis. 2019;6 (4):398–406.

[12] Xue Q, Yang, LP, Wang, H, et al. Silence of long noncoding RNA SNHG14 alleviates ischemia/reperfusion-induced acute kidney injury by regulating miR-124-3p/MMP2 axis. Biomed Res Int. 2021;2021:8884438.

[13] Huo Y, Zhao, K, Zhang, T, et al. MiR-124-3p alleviates the dezocine tolerance against pain by regulating TRAF6 in a rat model. Neuroreport. 2021;32(1):44–51.

[14] Dou Y, Tian, XD, Zhang, J, et al. Roles of TRAF6 in central nervous system. Curr Neuropharmacol. 2018;16 (9):1306–1313.

[15] Dong S, Zhang, Q, Kong, DL, et al. Gender difference in the effect of progesterone on neonatal hypoxic/ischemic brain injury in mouse. Exp Neurol. 2018;306:190–198.

[16] Li T, Qin, JJ, Yang, X, et al. The ubiquitin E3 ligase TRAF6 exacerbates ischemic stroke by ubiquitinating and activating Rac1. J Neurosci. 2017;37(50):12123–12140.

[17] Li HY, He, HC, Song, JF, et al. Bone marrow-derived mesenchymal stem cells repair severe acute pancreatitis by secreting miR-181a-5p to target PTEN/Akt/TGF-beta1 signaling. Cell Signal. 2020;66:109436.

[18] Fang S, Li Y, Chen P. Osteogenic effect of bone marrow mesenchymal stem cell-derived exosomes on steroid-induced osteonecrosis of the femoral head. Drug Des Devel Ther. 2019;13:45–55.

[19] Li T, Zhang, CF, Ding, YL, et al. Umbilical cord-derived mesenchymal stem cells promote proliferation and migration in MCF-7 and MDA-MB-231 breast cancer cells through activation of the ERK pathway. Oncol Rep. 2015;34(3):1469–1477.

[20] Qi X, Zhang, JY, Yuan, H, et al. Exosomes secreted by human-induced pluripotent stem cell-derived mesenchymal stem cells repair critical-sized bone defects through enhanced angiogenesis and osteogenesis in osteoporotic rats. Int J Biol Sci. 2016;12 (7):836–849.

[21] Xiao B, Zhu, YQ, Huang, JF, et al. Exosomal transfer of bone marrow mesenchymal stem cell-derived miR-340 attenuates endometrial fibrosis. Biol Open. 2019;8(5 1–9).

[22] Gangadaran P, Rajendran, RL, Lee, HW, et al. Extracellular vesicles from mesenchymal stem cells activates VEGF

receptors and accelerates recovery of hindlimb ischemia. J Control Release. 2017;264:112–126.

[23] Zhou X, Chu, XL, Yuan, HT, et al. Mesenchymal stem cell derived EVs mediate neuroprotection after spinal cord injury in rats via the microRNA-21-5p/FasL gene axis. Biomed Pharmacother. 2019;115:108818.

[24] Fang H, Li, HF, He, MH, et al. Long non-coding RNA MALAT1 sponges microRNA-429 to regulate apoptosis of hippocampal neurons in hypoxic-ischemic brain damage by regulating WNT1. Brain Res Bull. 2019;152:1–10.

[25] Chen WB, Zhang, LX, Zhao, YK, et al. C/EBPalpha-mediated transcriptional activation of miR-134-5p entails KPNA3 inhibition and modulates focal hypoxic-ischemic brain damage in neonatal rats. Brain Res Bull. 2020;164:350–360.

[26] Hu Q, Manaenko, A, Bian, HT, et al. Hyperbaric oxygen reduces infarction volume and hemorrhagic transformation through ATP/NAD(+)/Sirt1 pathway in hyperglycemic middle cerebral artery occlusion rats. Stroke. 2017;48(6):1655–1664.

[27] Zuo X, Luo, JF, Manaenko, A, et al. MicroRNA-132 attenuates cerebral injury by protecting blood-brain-barrier in MCAO mice. Exp Neurol. 2019;316:12–19.

[28] Fard N, Saffari, A, Emami, G, et al. Acute respiratory distress syndrome induction by pulmonary ischemia-reperfusion injury in large animal models. J Surg Res. 2014;189(2):274–284.

[29] Nemery B, Vanlommel, S, Verbeken, EK, et al. Lung injury induced by paraquat, hyperoxia and cobalt chloride: effects of ambroxol. Pulm Pharmacol. 1992;5 (1): 53–60.

[30] Qian D, Wei, G, Xu, CL, et al. Bone marrow-derived mesenchymal stem cells (BMSCs) repair acute necrotized pancreatitis by secreting microRNA-9 to target the NF-kappaB1/p50 gene in rats. Sci Rep. 2017;7(1):581.

[31] Zhang M, Ge, GD, Su, Z, et al. miR-137 alleviates focal cerebral ischemic injury in rats by regulating JAK1/STAT1 signaling pathway. Hum Exp Toxicol. 2020;39 (6):816–827.

[32] Zhu L, Zhou, XY, Li, SS, et al. miR1835p attenuates cerebral ischemia injury by negatively regulating PTEN. Mol Med Rep. 2020;22(5):3944–3954.

[33] Khan-Malek R, Wang Y. Statistical analysis of quantitative RT-PCR results. Methods Mol Biol. 2017;1641:281–296.

[34] Wang SL, Duan, L, Xia, B, et al. Dexmedetomidine preconditioning plays a neuroprotective role and suppresses TLR4/NF-kappaB pathways model of cerebral ischemia reperfusion. Biomed Pharmacother. 2017;93: 1337–1342.

[35] Yu Y, Zhang, XH, Han, ZG, et al. Expression and regulation of miR-449a and AREG in cerebral ischemic injury. Metab Brain Dis. 2019;34(3):821–832.

[36] Liu J, Zhang, S, Huang, YY, et al. miR-21 protects neonatal rats from hypoxic-ischemic brain damage by targeting CCL3. Apoptosis. 2020;25(3–4):275–289.

[37] Jiang X, Lew, KS, Chen, QY, et al. Human mesenchymal stem cell-derived exosomes reduce ischemia/reperfusion injury by the inhibitions of apoptosis and autophagy. Curr Pharm Des. 2018;24(44):5334–5341.

[38] Zhao Y, Gan, YX, Xu, GW, et al. MSCs-derived exosomes attenuate acute brain injury and inhibit microglial inflammation by reversing CysLT2R-ERK1/2 mediated microglia M1 polarization. Neurochem Res. 2020;45(5):1180–1190.

[39] Thomi G, Joerger-Messerli, M, Haesler, V, et al. Intranasally administered exosomes from umbilical cord stem cells have preventive neuroprotective effects and contribute to functional recovery after perinatal brain injury. Cells. 2019;8(8 855).

[40] Liu X, Zhang, MM, Liu, HN, et al. Bone marrow mesenchymal stem cell-derived exosomes attenuate cerebral ischemia-reperfusion injury-induced neuroinflammation and pyroptosis by modulating microglia M1/M2 phenotypes. Exp Neurol. 2021;341:113700.

[41] Safakheil M, Safakheil H. The effect of exosomes derived from bone marrow stem cells in combination with rosuvastatin on functional recovery and neuroprotection in rats after ischemic stroke. J Mol Neurosci. 2020;70(5):724–737.

[42] Liang YP, Liu, Q, Xu, GH, et al. The lncRNA ROR/miR-124-3p/TRAF6 axis regulated the ischaemia reperfusion injury-induced inflammatory response in human cardiac myocytes. J Bioenerg Biomembr. 2019;51(6):381–392.

[43] Chen F, Hu, Y, Xie, YT, et al. Total glucosides of paeony alleviate cell apoptosis and inflammation by targeting the long noncoding RNA XIST/MicroRNA-124-3p/ITGB1 axis in renal ischemia/reperfusion injury. Mediators Inflamm. 2020;2020:8869511.

[44] Vuokila N, Lukasiuk, K, Bot, AM, et al. miR-124-3p is a chronic regulator of gene expression after brain injury. Cell Mol Life Sci. 2018;75(24):4557–4581.

[45] Huang S, Ge, XT, Yu, JW, et al. Increased miR-124-3p in microglial exosomes following traumatic brain injury inhibits neuronal inflammation and contributes to neurite outgrowth via their transfer into neurons. FASEB J. 2018;32(1):512–528.

[46] Wang Y, Chen, G, Yu, XD, et al. Salvianolic acid B ameliorates cerebral ischemia/reperfusion injury through inhibiting TLR4/MyD88 signaling pathway. Inflammation. 2016;39(4):1503–1513.

[47] Zhao J, Zhang, XJ, Dong, LP, et al. Cinnamaldehyde inhibits inflammation and brain damage in a mouse model of permanent cerebral ischaemia. Br J Pharmacol. 2015;172(20):5009–5023.